International Atomic Energy Agency

INDC(GDR)-20
Distribution: L

INDC INTERNATIONAL NUCLEAR DATA COMMITTEE

INDC(GDR)-20

Description of the Evaluated Neutron Nuclear Data File 2015 for Silicon of the SOKRATOR Library

compiled by

D. Hermsdorf

Technical University of Dresden

July 1982

IAEA NUCLEAR DATA SECTION, WAGRAMERSTRASSE 5, A-1400 VIENNA

Printed by the IAEA in Austria
July 1983
83-03742

INDC(GDR)-20

Description of the evaluated neutron nuclear data file 2015 for Silicon of the SOKRATOR library

compiled by

D. Hermsdorf

Technical University of Dresden

July 1982

Preface

This paper describes the contents of file 2015 for Silicon of the Soviet library of evaluated neutron nuclear data SOKRATOR and the methods used for evaluation. Especially the experimental and calculated results chosen for nuclear data recommendations will be discussed. The numerical figures obtained have been formatted in ENDF/B-V format.

The editor would like to acknowledge Prof. Dr. D. Seeliger for his continuous interest in this work and his stimulating discussions. Also Drs. A.V. Ignatyuk and S. Cierjacks are gratefully thanked for reading the manuscript and for valuable remarks for the final version of this report.

Finally, the technical assistance of Mrs. P. Reichelt, S. Eckstein, R. Prengel and B. Krause in preparing the data file and this report should be emphasized and acknowledged.

Table of contents

Part A:

Intercomparison of evaluated neutron nuclear data files for Silicon

D. Hermsdorf

1. Introduction

From the World Request List for Nuclear Data (WRENDA) increasing demands for neutron nuclear data for Silicon were reported /1/. Especially requests for differential data (angular distributions and energy spectra) for neutron, charged particle and γ-ray emission have been compiled. Such data are necessary for investigations of changes of the material properties of Silicon caused by intense fast neutron fields, which will be especially produced by fusion reactors.
Furthermore, a principal interest in these data arise from safeguards and radiation shielding calculations.
In the international data exchange as well as experimental data (EXFOR) and evaluated data sets are available. This large amount of data should be examined to meet the requests compiled recently.

First of all, the aptitude, reliability and completeness of recommended data sets should be tested.

2. Analysis and intercomparison of evaluated nuclear data files for Silicon

At that time the analysis was going on data files for Silicon were available from following libraries:

UKNDL, ENDL, ENDF/B, JENDL, SAND-II and SOKRATOR.

The data have been processed by computer codes of our data managing system DAPROC in order to list the contents and to prepare the graphical display of all data /2/.

From this following informations should be listed:

i) UKNDL

status : DFN 25 E is a very old file published 1964 /3/; also accepted for the version UKNDL-80 /4/;

contents: integral neutron data; differential data for neutrons only (angular distributions of elastically scattered neutrons);

remarks : most discrepant data in comparison with more recent files; should be used with caution only.

ii) ENDL

status : appeared in 1972 as ENDL-2 MAT 7120 /5/; no changes in data for versions ENDL-76 (MAT 7120) and ENDL-78 (MAT 7820);

contents: including energy spectra for neutrons also;

remarks : none

iii) ENDF/B

status : version III (MAT 1151) from 1973 /6/ has been improved considerably to give version IV (MAT 1194) in 1979;

contents: complete file including γ-ray and charged-particle data also;

remarks : the improved version V was not available for comparison.

iv) JENDL

status : version 1 (MAT 1140) appeared 1979 /7/;

contents: only neutron integral and differential data; taken from ENDF/B-IV mainly;

remarks : version 2 in preparation but not available at that time the present work has been done.

v) <u>SAND-II</u>

status : multi-group library for dosimetry purposes /8/ established in 1970;

contents : only excitation functions for (n,p) and (n,α);

remarks : deviations to the most refined evaluated data from ENDF/B-IV; should be used with caution.

vi) <u>SOKRATOR</u>

status : angular distributions for elastic neutron scattering have been evaluated by Bazazyanc in 1972 /9/;

contents : Legendre polynomials expansion coefficients of elastic scattering only;

remarks : difficulties appear in use of a limited number of coefficients for parametrization of strongly oscillating angular distributions (negative cross sections at minima).

Some pictures (figs. 1 to 5) have been selected to demonstrate discrepancies also in evaluated data sets which have been created to be used as "best" data. Other examples will be shown in the corresponding paragraphs of this paper.

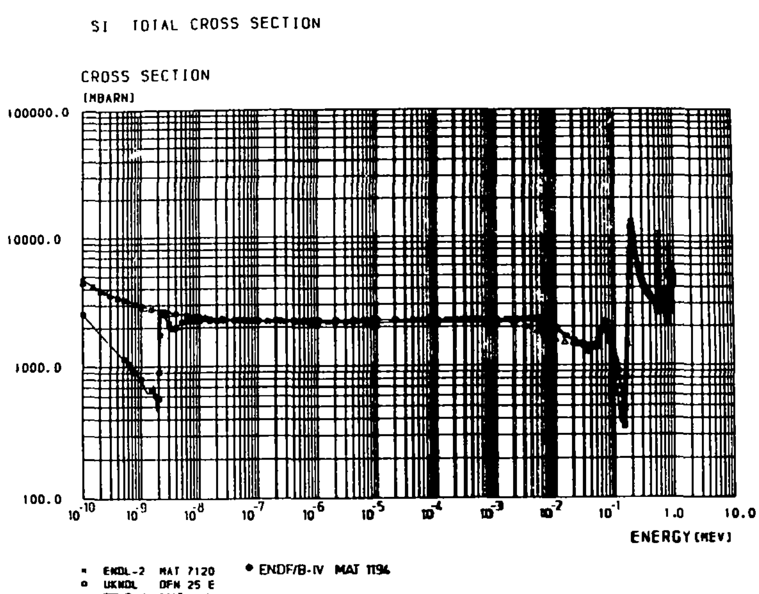

Fig. 1

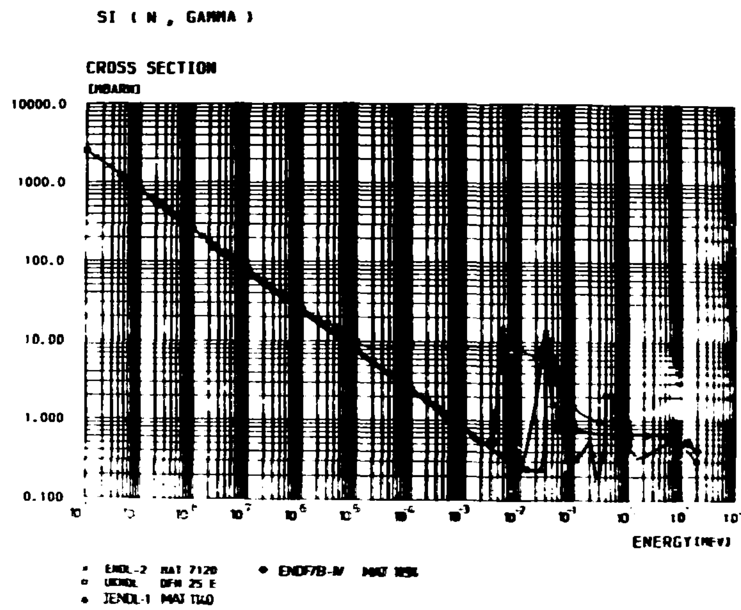
SI (N , GAMMA)
CROSS SECTION
(MBARN)
10000.0
1000.0
100.0
10.00
1.000
0.100
ENERGY(MEV)
ENDL-2 MAT 7120
UKNDL DFN 25 E
JENDL-1 MAT 1140
ENDF/B-IV MAT 1194

Fig. 2

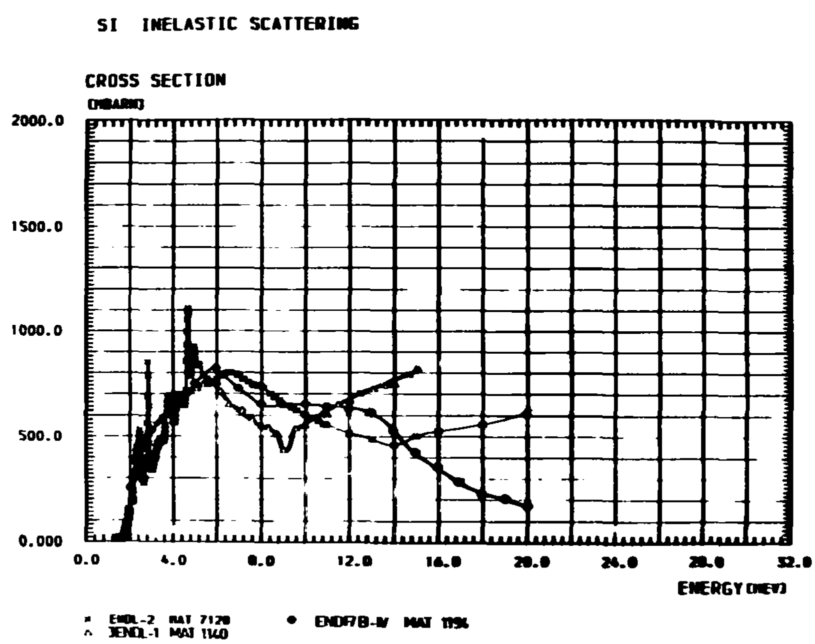
SI INELASTIC SCATTERING
CROSS SECTION
(MBARN)
2000.0
1500.0
1000.0
500.0
0.000
0.0
4.0
8.0
12.0
16.0
20.0
24.0
28.0
32.0
ENERGY(MEV)
ENDL-2 MAT 7120
JENDL-1 MAT 1140
ENDF/B-IV MAT 1194

Fig. 3

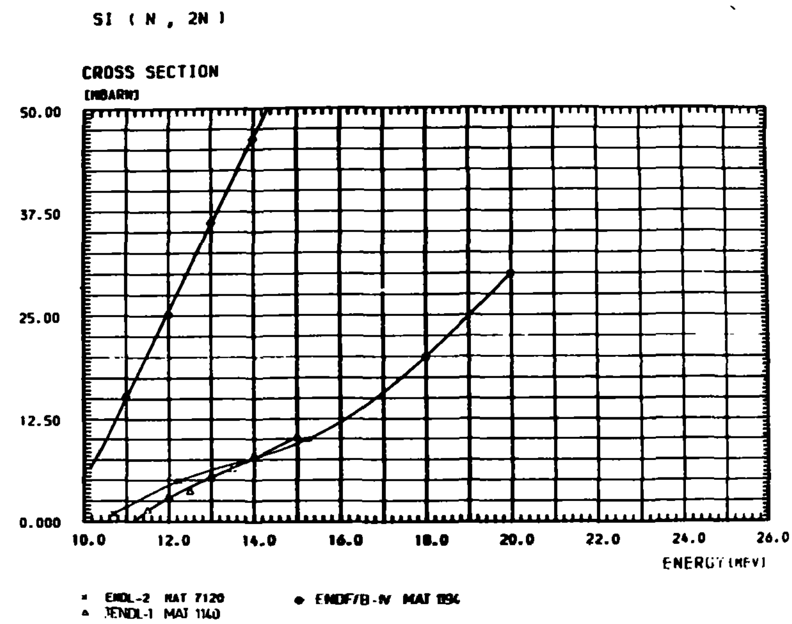
SI (N , 2N)
CROSS SECTION
[MBARN]
50.00
37.50
25.00
12.50
0.000
10.0
12.0
14.0
16.0
18.0
20.0
22.0
24.0
26.0
ENERGY (MEV)
ENDL-2 MAT 7120
JENDL-1 MAT 1140
ENDF/B-IV MAT 1194

Fig. 4

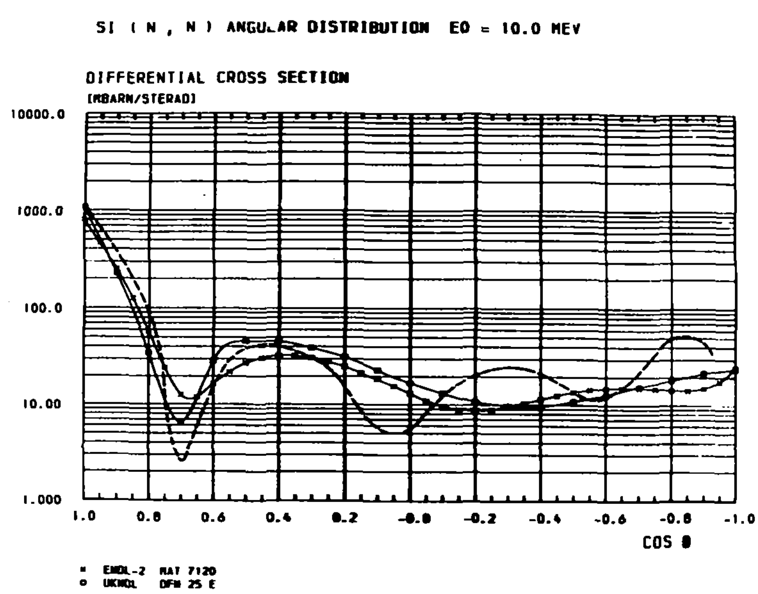
SI (N , N) ANGULAR DISTRIBUTION E0 = 10.0 MEV
DIFFERENTIAL CROSS SECTION
[MBARN/STERAD]
10000.0
1000.0
100.0
10.00
1.000
1.0
0.8
0.6
0.4
0.2
-0.0
-0.2
-0.4
-0.6
-0.8
-1.0
COS θ
ENDL-2 MAT 7120
UKNDL DFN 25 E
Bazazyanc

Fig. 5

3. Results and conclusions

Abstracting from all details of the results obtained from the intercomparison of recommended data following four points can be concluded:

i) there is no really independent evaluation later than 1975 roughly;

ii) recommended data strongly deviate in nearly all quantities given in the files;

iii) new experiments published recently can be included to clear discrepancies;

iv) a recommended nuclear data file should not be a complete file only but also as flexible as possible against different purposes.

These arguments substantiate the decision to create a new evaluated data set more than an improvement of a file available at present.

Finally, all numerical results have to be compressed and checked against inconsistencies in partial and total cross sections. After that the data set will be coded in the ENDF/B-V format for convenience of international exchange.

4. References

/1/ D.W. Muir,
WRENDA 79/80, INDC(SEC)-73/URSF, 1979;
N. Day Day,
WRENDA 81/82, INDC(SEC)-78/URSF, 1981;
Nuclear Data for Fusion Research Reactor Technology,
IAEA-TECDOC-223, 1979

/2/ D. Hermsdorf, D. Seeliger, Kernenergie 23 (1980)285

/3/ Barrington, report AERW-R-351, 1964

/4/ O. Schwerer, report IAEA-NDS-30, Rev. 0, 1980

/5/ R. Howerton, report UCRL-50400, Vol. 15, Part A, 1975

/6/ M.R. Bhat, report BNL-50379, 1973

/7/ S. Igarasi et al., report JAERI-1261, 1979

/8/ R.L. Simsons, W.A. McElroy, report BNWL-1312, 1970

/9/ N.O. Bazazyanc et al., Yad. Konst. 8 (1972) 61

5. Figure captions

Fig. 1 Silicon total cross section.
The overall agreement of evaluated data files ENDF/B-IV, ENDL-2, UKNDL and JENDL-1 is satisfactory. Lattice effects will be taken into account by UKNDL only.

Fig. 2 Silicon capture cross section.
Recommended data by ENDF/B-IV, ENDL-2, UKNDL and JENDL are most discrepant in the energy range from 10^{-5} to 20 MeV.

Fig. 3 Silicon neutron inelastic scattering cross section.
Recommended data by ENDF/B-IV, ENDL-2 and JENDL-1 diverge above 6 MeV considerably.

Fig. 4 Si(n,2n) cross section.
Discrepancies between ENDF/B-IV, ENDL-2 and JENDL-1 are caused by the influence of ^{29}Si(n,2n) to the total (n,2n) cross section taken into account by ENDF/B-IV only.

Fig. 5 Si(n,n) differential cross section at 10 MeV neutron incident energy.
Recommended data by ENDL-2, UKNDL and SOKRATOR (evaluated by Bazazyanc) give different oscillating structures.

Part B:

Neutron total cross sections and resonance parameters

D. Hermsdorf, H. Philipp

1. Review of experimental data base

The total cross section for neutrons on natural Silicon is the most intensive investigated quantity considered in the course of this evaluation. Experimental data have been obtained from 28 authors /1 to 28/ in the neutron incident energy range from 10^{-9} to 100 MeV. The quality of the measurements are quite different resulting from different neutron sources, energy resolution and other measuring conditions.

At lowest energies deviations from an expected smooth dependence on energy can be observed caused by incoherent neutron scattering. Rustad's /11/ measurement in fig. 1 demonstrates this effect to appear at about $2.0 \cdot 10^{-9}$ MeV (or λ = 1.02 Å) corresponding to the well-established lattice spacing d=1.045 Å for [511] and [333] orientation.

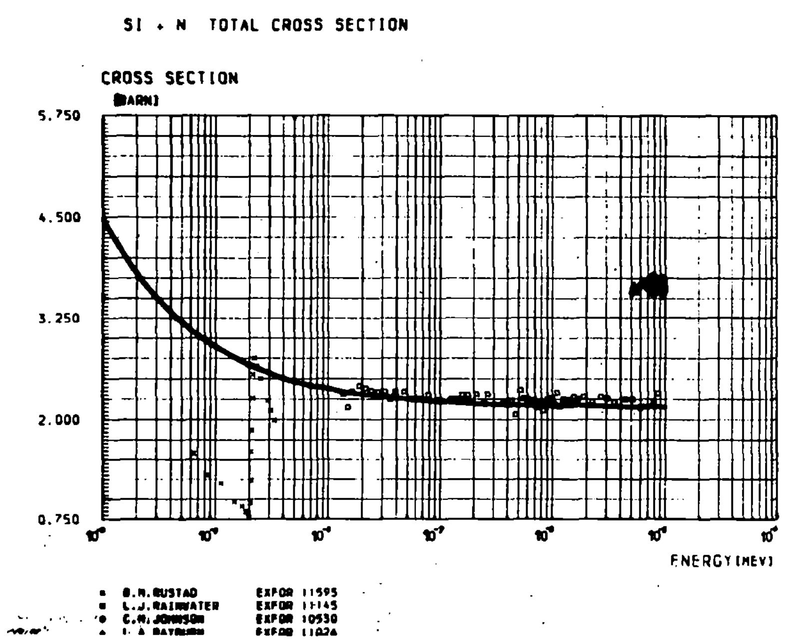

Fig. 1

Up to an energy of about 10^{-1} MeV a flat energy dependence is realized which can be understood in terms of simple potential scattering in absence of any resonance and only a very small contribution from neutron capture.

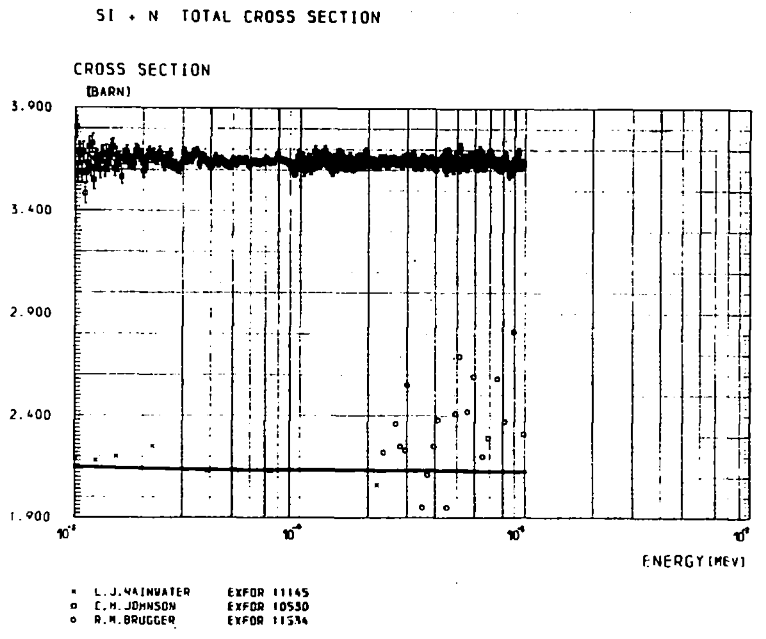
SI + N TOTAL CROSS SECTION
CROSS SECTION
(BARN)
3.900
3.400
2.900
2.400
1.900
ENERGY (MEV)
L.J.RAINWATER EXFOR 11145
C.M.JOHNSON EXFOR 10530
R.M.BRUGGER EXFOR 11534

Fig. 2

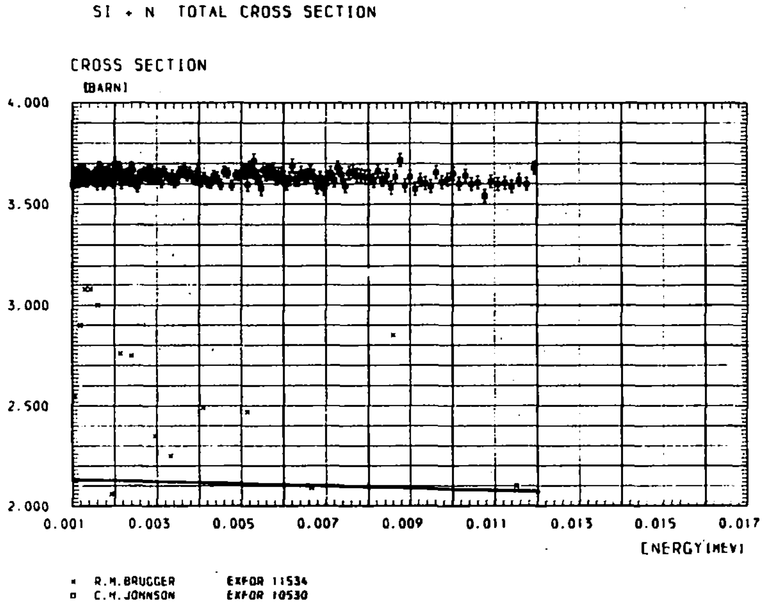
SI + N TOTAL CROSS SECTION
CROSS SECTION
(BARN)
4.000
3.500
3.000
2.500
2.000
0.001
0.003
0.005
0.007
0.009
0.011
0.013
0.015
0.017
ENERGY (MEV)
R.M.BRUGGER EXFOR 11534
C.M.JOHNSON EXFOR 10530

Fig. 3

From figs. 2 and 3 it is evident that Johnson's /8/ data are so discrepant in magnitude to have to be excluded from further considerations. On the other hand there are not enough data in the energy range from 10^{-2} to 10^{-1} MeV to substantiate the appearance of any resonance obtained by that author.

The first well-established resonance found by Whalen /4/ appears at 0.1865 MeV (fig. 4).

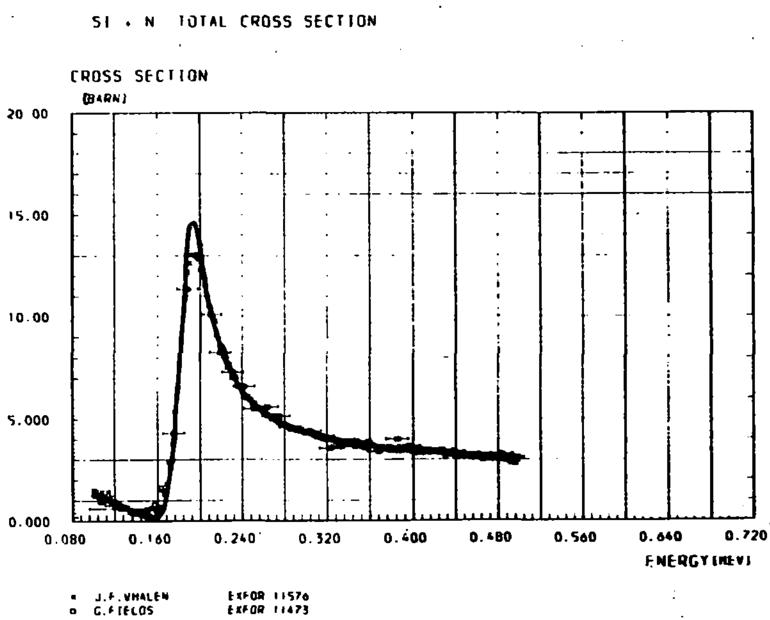

Fig. 4

Above 0.5 MeV neutron incident energy a large amount of experimental data exist. Mainly the authors Cierjacks /1/, Schwartz /2/ and Perey /3/ may be refered. Comparing the results of these authors a satisfactory agreement can be confirmed around 0.5 MeV in absolute value and resonance structure found.

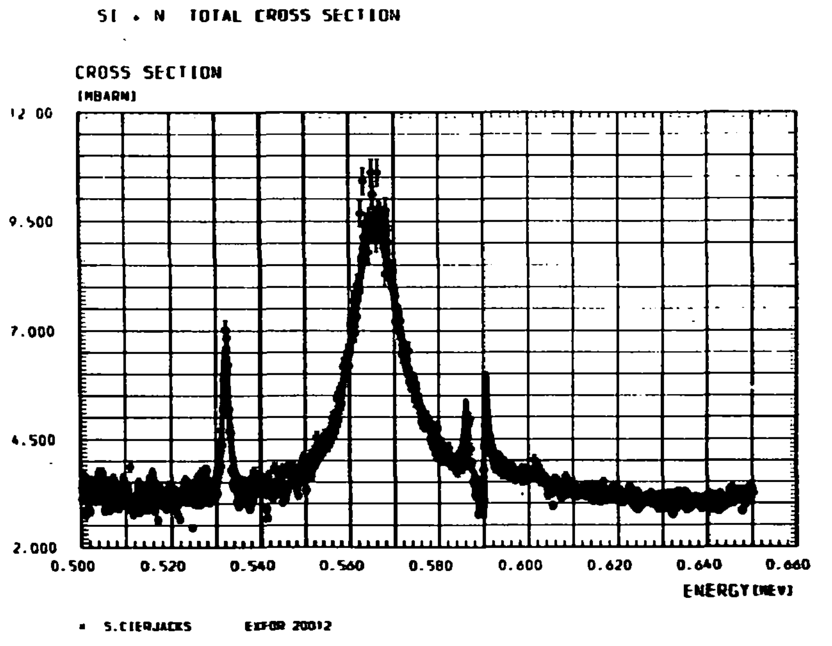
SI + N TOTAL CROSS SECTION
CROSS SECTION
(MBARN)
12.00
9.500
7.000
4.500
2.000
0.500
0.520
0.540
0.560
0.580
0.600
0.620
0.640
0.660
ENERGY(MEV)
S.CIERJACKS
EXFOR 20012

Fig. 5

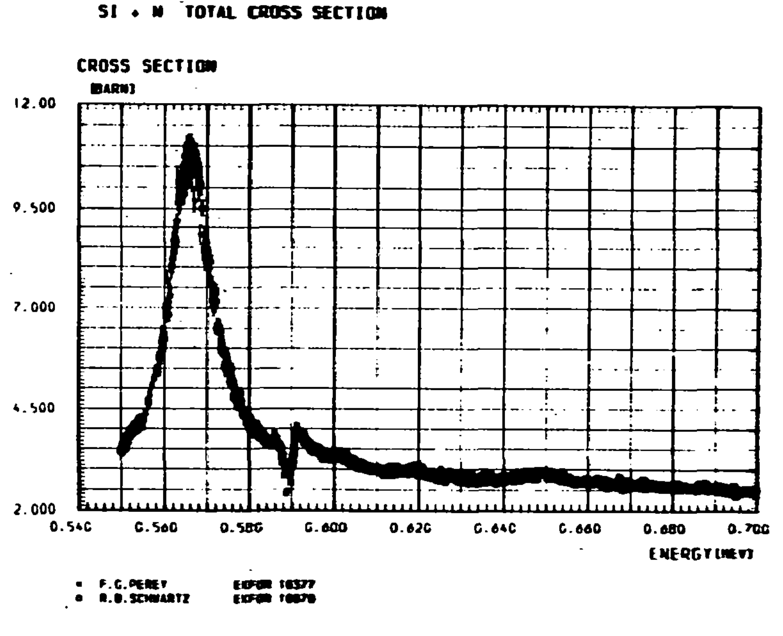
SI + N TOTAL CROSS SECTION
CROSS SECTION
(BARN)
12.00
9.500
7.000
4.500
2.000
0.540
0.560
0.580
0.600
0.620
0.640
0.660
0.680
0.700
ENERGY(MEV)
F.G.PEREY
R.B.SCHWARTZ

Fig. 6

With increasing energy the resonances determined by these authors differ to some extent in energy and maximum cross section. It should be noted that Cierjacks' measurement yields higher cross sections up to about 10 % at 0.7 MeV in comparison to Schwartz and Perey. However, this divergence loses with increasing energy.

Comparing other experimental results in the 1 MeV energy range very discrepant data as well as in magnitude and structure can be observed. So, the data obtained by Whalen /4/, Cox /5/, Freier /6/, Fields /7/ and Johnson /8/ have been excluded in the present evaluation.

Around 10 MeV the measured data of Cierjacks, Schwartz and Perey agree very well within the confidence of the experiments (in the order of 4 %) seen in fig. 7.

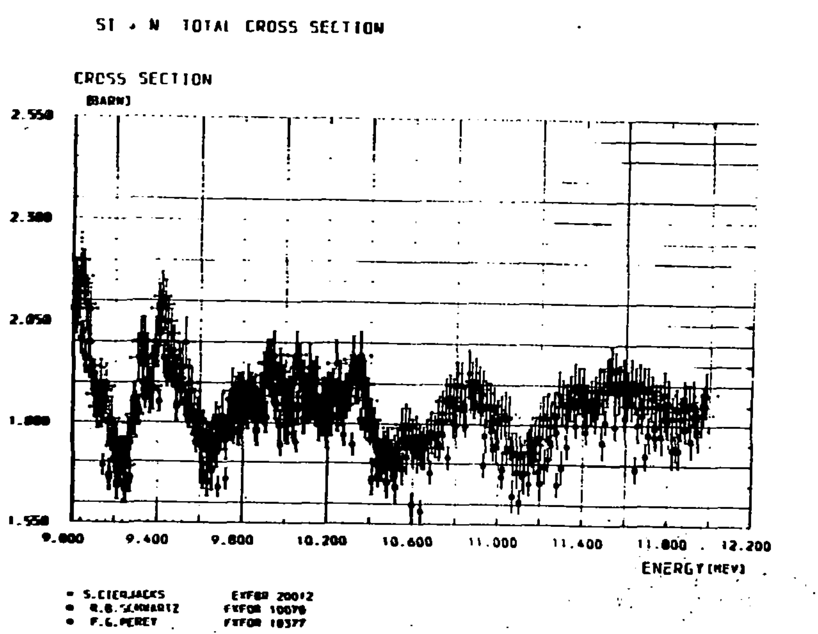

Fig. 7

With further increasing energy the intermediate structure will be smeared out by worser energy resolution of the experiments as well as from physics aspects. Around 20 MeV the most reliable experimental data diverge to such an extend that there is no overlapping within the errors given by authors (fig. 8).

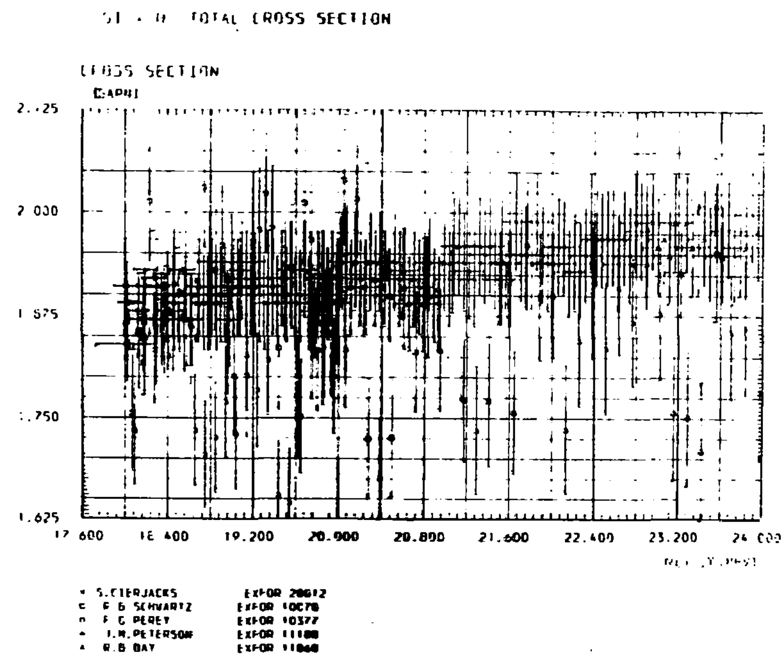

Fig. 8

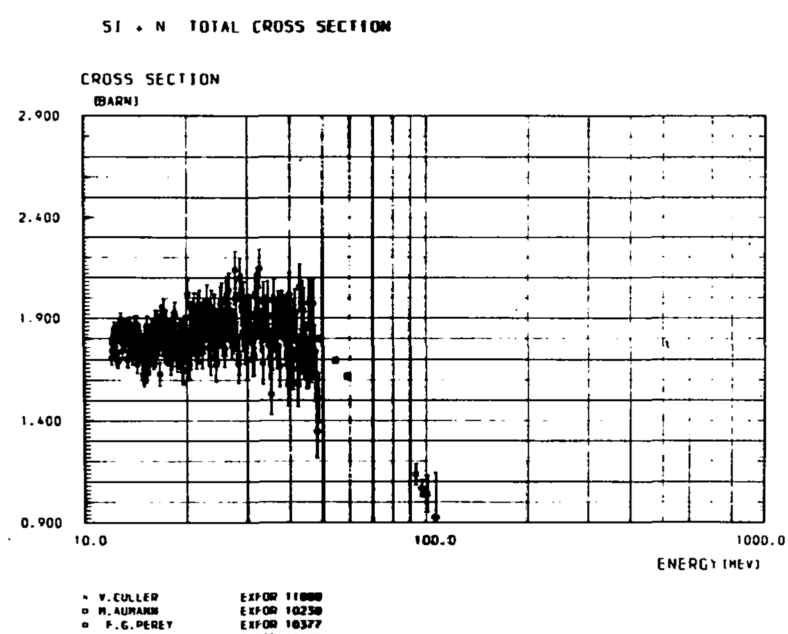

Fig. 9

To complete the discussion,the energy range from 20 to 100 MeV may be reviewed briefly. Several authors /3, 21, 25, 26/ have published data which scatter considerably. Typical errors of measurements are in the order 15 to 20 % as it is demonstrated in fig. 9.

In the energy range of interest for an evaluation, i.e. 10^{-5}eV to 20 MeV, the measurements of Rustad /11/, Rainwater /12/, Brugger /13/, Fields /7/, Whalen /4/ and Cierjacks /1/ have been choosen to be the most reliable and consistent data sets. Basing on these data an analysis has been performed.

2. Analysis of the total cross section

2.1. Interpretation of resonance structure

Comparing figs. 1 to 3 it can obviously seen that the energy range from 10^{-5} eV up to 10 keV may be used to fit the potential scattering radius. Taking into account a contribution of neutron capture by 0.0235046 $/\sqrt{E/eV}$ barns the superposition yields a value a_p=4.985 fm. Calculated results are included in figs. 1 to 3 as solid line.

Proceeding from present status of experimental informations the resonances between 10 keV and 100 keV summarized in other compilations /29/ and evaluations /30/ could not confirmed. For further clear up table 1 presents resonance parameters found in literature.

Above 100 keV the high-resolution experiments of Whalen /4/, Fields /7/ and Cierjacks /1/ have been interpreted in terms of the Single-Level-Breit-Wigner-Formalism (SLBW) defined in the description of ENDF/B-format /31/. Starting from resonance parameters in an iterative procedure "best fit" parameters were obtained tabulated in table 2. Results can be seen in figs. 5, 10 and 11. The simple SLBW method is limited clearly by the existence of level-level-inferences (also seen in figs. 10 and 11) above 1.5 MeV.

Better fits can be obtained using Multi-Level-formulae basing on R-matrix-theory. Such an analysis has been done by Cierjacks /32/.

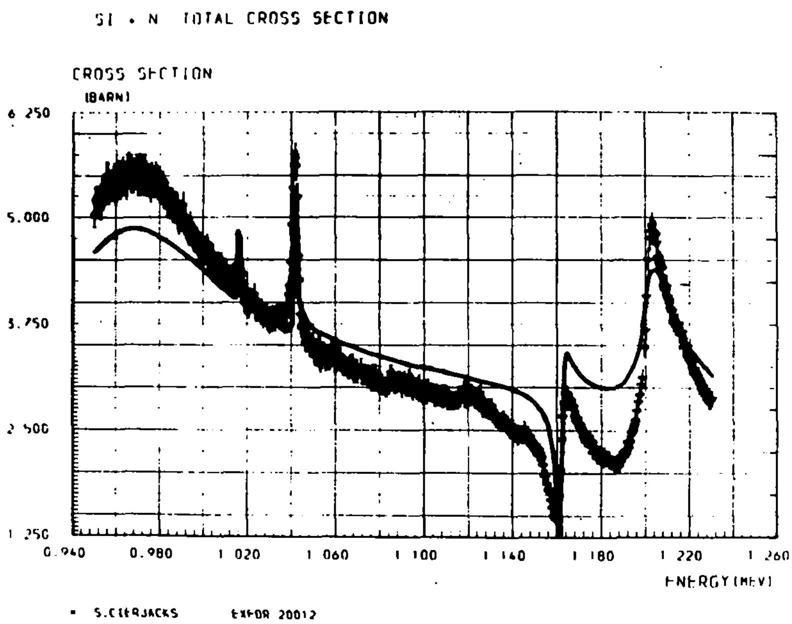

Fig. 10

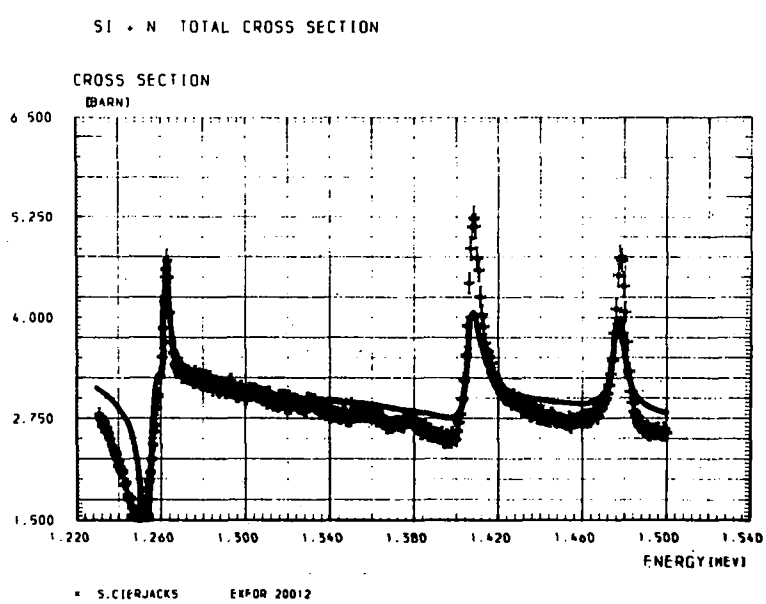

Fig. 11

2.2. Interpretation of intermediate and gross structure

Above 1.56 MeV the use of the SLBW-Formalism results in worse description of the experimental data. In default of a Multi-Level-Formalism only a simple averaging procedure has been applied to interprete the total cross sections up to 20 MeV. Experimental data of Cierjacks /1/ were smoothed by folding with a Gaussian shaped form factor of a width equal to the experimental resolution. From this method real intermediate structure may be maintained.

3. Calculation of total cross sections in terms of the optical model

The prediction of neutron total cross sections by the optical model is not the most sensitive but nevertheless an important test of the potential parameters applied. Using the parameter set resulting from a consistent interpretation of differential elastic neutron scattering (described in Part C) total cross sections have been calculated in the whole energy range under consideration. The overall agreement is fairly well for energies above 1 MeV (see fig. 12). The tendency to predict smaller total cross sections up to 7 % at 20 MeV should be noted. This may arise from the use of an energy-indepent imaginary potential.

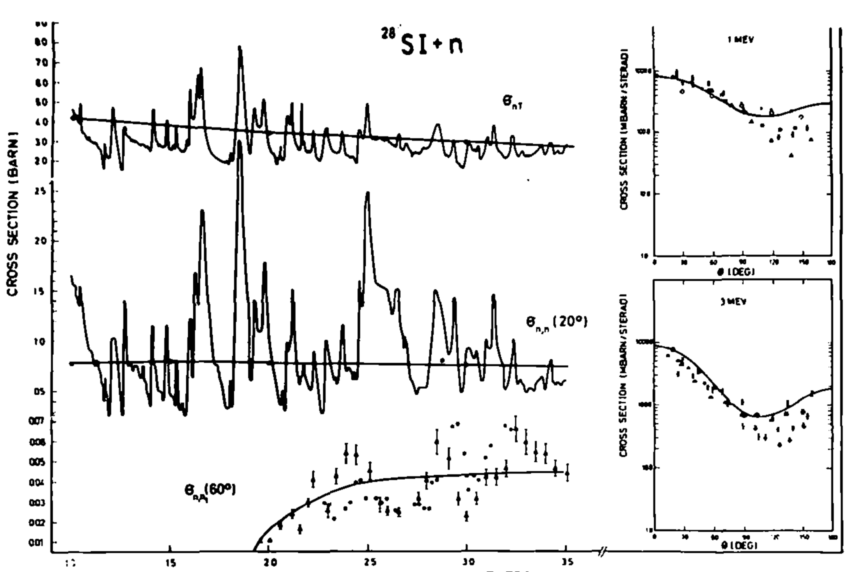

Fig. 12

4. Conclusions and recommendations

The success of an interpretation of total cross sections from 10^{-5} eV up to 1.56 MeV in terms of the SLBW-method leads to the representation in resonance parameters (File 2) and a "background" (File 3) containing residual quantities $\sigma^{res}_{nT} = \sigma^{exp}_{nT} - \sigma^{theor.}_{nT}$.

Residuals as well as averaged cross sections in the range from 1.56 to 20 MeV has been transformed in the nuclear data format ENDF/B-V /33/ automatically using computer codes from the code package for EXFOR data handling DAPROC /34/.

5. References

/1/ S. Cierjacks et al., report KFK-1000, 1968

/2/ R.B. Schwartz et al., Bull. Am. Phys. Soc. 16 (1971) 495

/3/ F.G. Perey et al., report ORNL-4823, 1972

/4/ J.F. Whalen et al., EXFOR accession no. 11576.002

/5/ S.A. Cox et al., EXFOR accession no. 11547.002

/6/ G. Freier et al., Phys. Rev. 78 (1950) 508

/7/ E.R. Fields et al., Phys. Rev. 83 (1951) 479

/8/ C.H. Johnson et al., report ORNL-5025, 1975

/9/ J. Cabe et al., EXFOR accession no. 20480.006

/10/ B.G. Foster et al., Phys. Rev. C3 (1971) 576

/11/ B.M. Rustad et al., report BNL-325, 1973

/12/ L.J. Rainwater et al., Phys. Rev. 73 (1948) 733

/13/ R.M. Brugger et al., EXFOR accession no. 11534.003

/14/ L.A. Rayburn et al., Nucl. Phys. 61 (1965) 381

/15/ N. Nereson et al., Phys. Rev. 89 (1953) 775

/16/ K. Tsukada et al., Jour. Phys. Japan 18 (1963) 610

/17/ F. Manero et al., Nucl. Phys. 65 (1965) 419

/18/ A.D. Carlson et al., Phys. Rev. 158 (1967) 1142

/19/ S.M. Grimes et al., Nucl. Phys. A124 (1969) 369

/20/ W.H. Zinn et al., Phys. Rev. 56 (1939) 260

/21/ J.M. Peterson et al., Phys. Rev. 120 (1960) 521

/22/ R.B. Day et al., Phys. Rev. 92 (1953) 358

/23/ K. Tsukada et al., EXFOR accession no. 20325.006 and .007

/24/ J.H. Coon et al., Phys. Rev. 88 (1952) 562

/25/ M. Auman et al., Phys. Rev. C5 (1972) 1

/26/ V. Culler et al., Phys. Rev. 99 (1955) 740

/27/ A.M.J. Spits et al., Nucl. Phys. A145 (1970) 449

/28/ A.M.J. Spits et al., Nucl. Phys. A224 (1974) 517

/29/ S.F. Mughabghab, D.I. Garber, report BNL-325, Vol. I, 1973

/30/ S. Igarasi, T. Nakagawa, Y. Kikuchi, T. Asami, T. Narita, report JAERI 1261, INDC(JAP)-45/L, 1979

/31/ D. Garber, C. Dunford, S. Pearlstein, report BNL-NCS-50496, ENDF 102, 1975

/32/ S. Cierjacks, private communication, 1982

/33/ S. Pearlstein, BNL-NCS-28949, suppl. ENDF 102, 2nd Edition, 1980

/34/ D. Hermsdorf, D. Seeliger, Kernenergie 23 (1980) 285

6. Tables

Table 1: Resonance parameters obtained for the energy range 10 keV to 100 keV not confirmed in the present evaluation

E_R/keV	l	J	Γ_n/eV	Γ_γ/eV	Γ/eV	reference
bound level	0	1/2	-	-	-	/29/
4.98	-	-	-	0.006	-	/29/
15.14	-	-	-	0.004	-	/29/
15.29	-	-	-	0.052	-	/29/
31.74	2	5/2	0.019	1	-	/30/
38.82	-	-	-	0.23	-	/30/
55.6± 0.2	0	1/2	1500± 300	0.54	-	/29/
55.9	0	1/2	1500	0.113	-	/30/
67.71	1	3/2	10	1.185	-	/30/
67.79± 0.2	1	-	-	1.64	-	/29/
70.84	-	-	-	0.03	-	/29/
70.8	2	2.1	0.015	1	-	/30/
86.98	-	-	-	0.30	-	/29/

Table 2: Resonance parameters for calculation of neutron total cross section, elastic scattering cross section and neutron capture in terms of the Single-Level-Breit-Wigner-Formalisms

E_R/MeV	l	J	Γ_n/eV	Γ_γ/eV
0.1865	0	1/2	29000	13.8
0.532	1	3/2	2000	0.8
0.5635	1	3/2	14000	-
0.5655	1	3/2	11000	4.0
0.5865	1	1/2	100	3.3
0.5899	0	1/2	200	-
0.602	1	1/2	30	4.1
0.771	1	1/2	100	4.0
0.8115	1	3/2	28000	-
0.8145	1	3/2	32000	20.8
0.8442	2	3/2	1500	7.0
0.8714	1	1/2	50	17.0
0.9096	1	3/2	6500	2.3
0.959	1	3/2	95000	4.8
1.016	1	3/2	200	-
1.0415	1	3/2	1500	-
1.1615	0	1/2	2500	-
1.202	1	3/2	15000	-
1.254	0	1/2	5000	-
1.263	1	3/2	2000	-
1.407	1	3/2	7000	-
1.477	2	5/2	7000	-
1.51	1	1/2	600	-
1.5275	1	3/2	6000	-

7. Figure captions

Fig. 1 Silicon total cross section.
The recommended data by present work (solid line) are basing on experimental data by Rainwater /12/.

Fig. 2 Silicon total cross section.
Evaluated data (solid line) in the energy range from 10^{-5} to 10^{-3} MeV will be substantiated by experimental ones by Rainwater /12/ and Brugger /13/.

Fig. 3 Silicon total cross section.
In the energy range from 10^{-3} to 10^{-2} MeV the evaluation (solid line) is supported by Brugger /13/.

Fig. 4 Silicon total cross section.
Evaluated data (solid line) is in agreement with experiments by Whalen /4/ and Fields /5/.

Fig. 5 Silicon total cross section.
High-resolution experiments by Cierjacks /1/ have been done in the range from about 0.5 to 25 MeV.

Fig. 6 Silicon total cross section.
In the energy range from 0.5 to 25 MeV other experiments by Perey /3/ and Schwartz /2/ are available for comparison with Cierjacks /1/.

Fig. 7 Silicon total cross section.
In the energy intervall from 9 to 12 MeV a reasonable agreement is achieved by the authors Cierjacks /1/, Schwartz /2/ and Perey /3/.

Fig. 8 Silicon total cross section.
In the energy intervall from 18 to 24 MeV the experimental data are in satisfactory agreement with the exception of data obtained by Perey /3/.

Fig. 9 Silicon total cross section.
Compilation of experimental data in the energy range from 20 to 100 MeV.

Fig. 10 Silicon total cross section.
The solid line represents the representation of experimental data by Cierjacks /1/ in terms of Single-Level-Breit-Wigner-Formalism.

Fig. 11 Same as in fig. 10.

Fig. 12 Silicon total cross section.
Measurements by Cierjacks /1/ (denoted by σ_{nT}) are compared with optical model calculations (solid line) using potential parameters compiled in table 1 of part C.

Part C:

Neutron scattering and production cross sections

D. Hermsdorf, L. Neumann, D. Seeliger

1. Neutron elastic scattering

1.1. Review of experimental data base

The angular distribution of elastically scattered neutrons has been extensively investigated by numerous experimentators /1 to 30/ in a very broad range of neutron incident energy from the keV-range up to 26 MeV /22/. A compilation of all reliable results is very important for the analysis of the energy dependence of differential elastic scattering cross sections in terms of the optical model.

General conclusions on the systematics of angular distributions from different measurements render more difficult by several reasons:

i) different energy resolutions achieved in measurements vary from 90 keV at 3 MeV /30/ to 700 keV at 10 MeV /21/ in dependence on measuring techniques and neutron sources. Therefore, the experimental averaging over the resonance structure (fig. 1) is very different from one experiment to the other. This results in spreading data at nearly the same neutron incident energy.

Fig.1

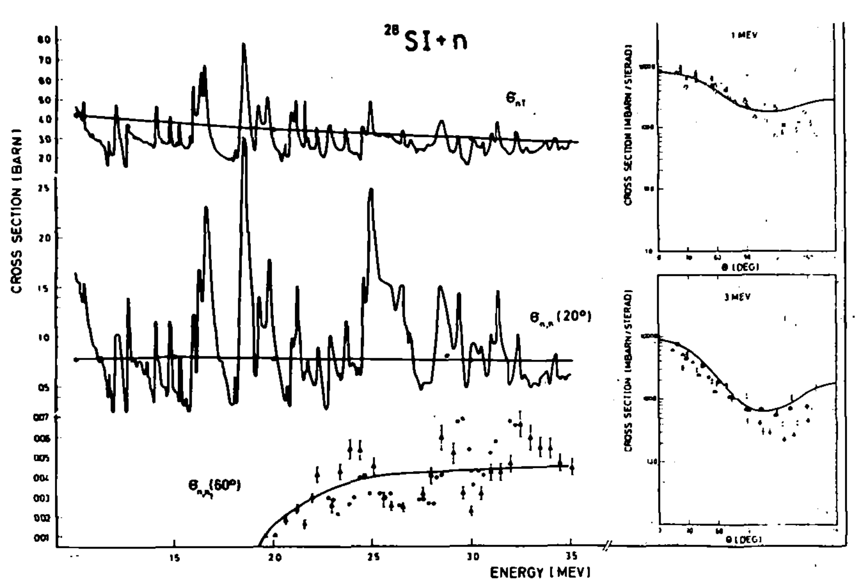

ii) angular dependences of the energy of produced neutrons by different sources especially for reactions with low Q-value results also in spreading of differential elastic scattering cross sections at backward angles mainly.

iii) the experimental data have been given as well as in the Lab system and the C-M-system non-uniformly causing deviations in the order of 5 % which can be corrected for.

iv) several authors don't obtain angular integrated cross sections. An integration procedure in terms of a Legendre polynomials expansion carried out subsequently results in ambig~~o~~uities at extreme forward and backward scattering angles caused by the limited range of angles investigated by that authors (normally from 30 to 150 degrees).

Fig. 2

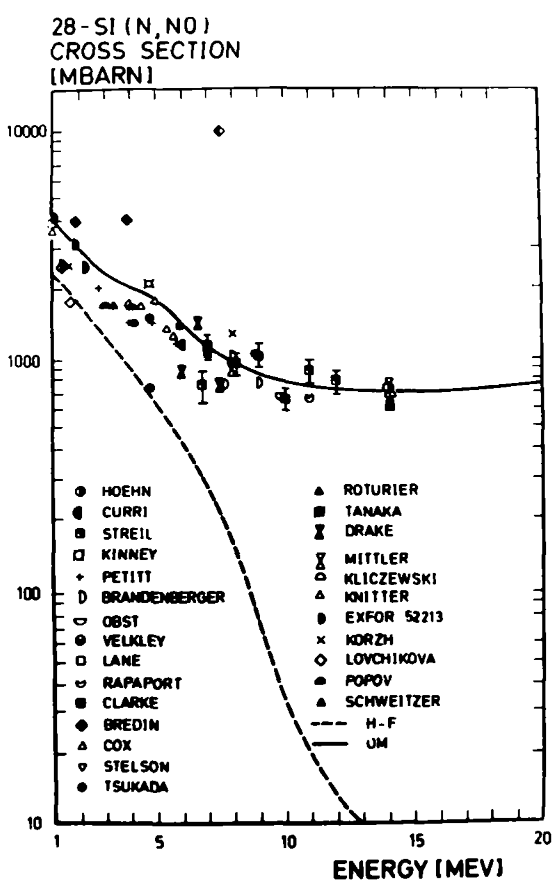

Summarizing these aspects, spreading data as well as for angular distributions and integral cross section (n,n_0) shown in fig. 2 are not surprisingly. The interpretation in terms of nuclear reaction models should take into account these physics phenomena.
Below about 1.5 MeV the elastic scattering cross sections have been determined very precisely as well as in the angular distributions and the integral values (fitting the structure in total cross sections nicely) by Schouky /29/ and Kinney /12/.

1.2. Theoretical interpretation of elastic scattering cross sections in terms of nuclear reaction models

1.2.1. Optical model analysis

Several optical potential parameter sets given by Bhat /31/, Holmqvist /32/, Obst /21/ and Kliczewski /25/ summarized in table 1 and other ones have been studied intensively to find the best one fitting all experimental data in the range from 1 to 26 MeV neutron incident energy /1 to 30/. A slightly modified version of Obst's potential well yields an optimum interpretation of all available data which is demonstrated by some examples (figs. 3 to 5).

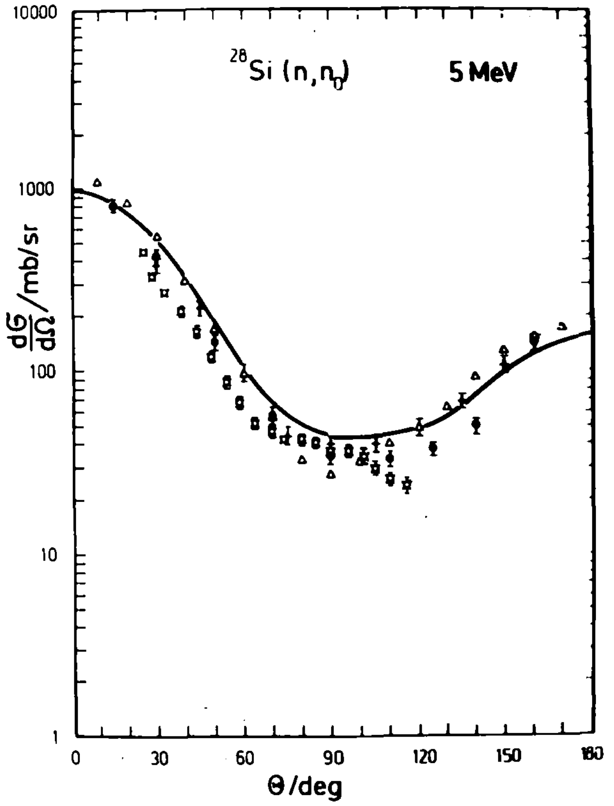

Fig. 3

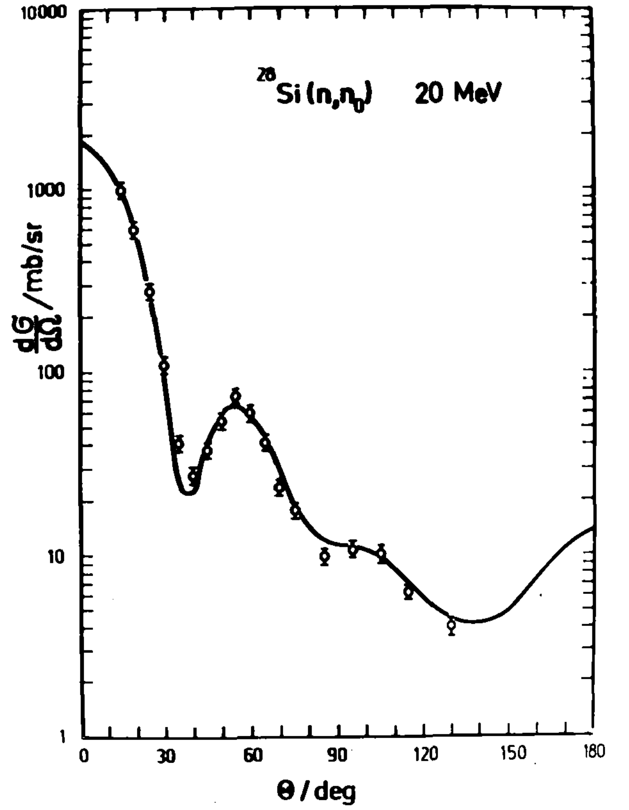

Fig. 4

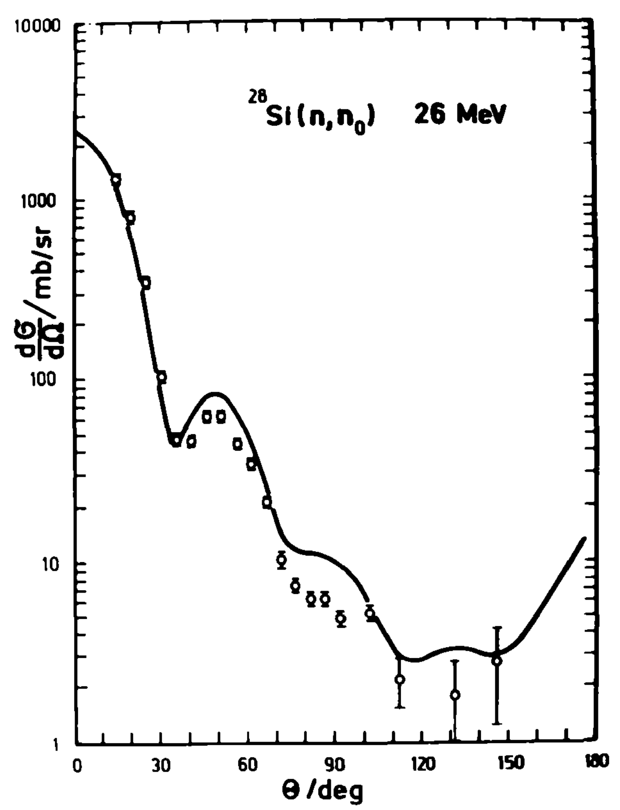

Fig. 5

1.2.2. Analysis of the compound elastic scattering

The adjustment of optical potential parameters described above has been done after subtracting contributions from compound elastic scattering which have been evaluated in terms of the Hauser-Feshbach-formalism properly using the computer code ELIESE-III /33/. This is an iterative procedure really and should be done two times at least.

Results of calculations in terms of optical and statistical model has been added incoherently to yield as well as differential and integrated elastic scattering cross sections shown in figs. 1 to 5 as solid line already. In fig. 2 the contribution of compound elastic scattering to the total elastic scattering cross section is given (dashed line) also. The expected significant amount of compound elastic scattering at low energies is confirmed.

1.3. Conclusions and recommendations

Generally, the experiments have been done using natural Silicon as target. On the other side, theoretical calculations can be done for isotopes only. But, taking into account contributions of the minor isotopes ^{29}Si (4.70 %) and ^{30}Si (3.09 %) the cross sections for the natural admixture will be negligible influenced in the order of about 0.5 to 1.5 %. Such a value can be considered to be within the accuracy of the models applied, the experimental errors of about 10 to 20 % and the re-adjustment necessary in any evaluation to obtain a consistent data set.

The representation of recommended data in the present evaluation is divided into two energy ranges. At the first one (10^{-5} eV up to 1.56 MeV) total elastic scattering data can be calculated according the Single-Level-Breit-Wigner-formalism taking parameters compiled in MF=2. From 1.56 to 20 MeV recommended total elastic scattering cross sections have been derived from the difference of total cross section and the proper adjusted non-elastic cross sections.

2. Neutron inelastic scattering

2.1. Review of experimental data

The experimental investigation of neutrons inelastically scattered on isotopes of Silicon is mainly restricted to measurements of the excitation of lowest-lying levels in ^{28}Si in angular distribution and integrated cross sections /4, 6, 7, 8, 10, 12, 14, 15, 17, 19, 20, 24, 25, 28, 34, 35/. On the other hand, experimental informations are very scarce for the excitation of level continuum of Si /36/ and absent totally for other isolated isotopes.

Further it should be noted that different authors have obtained very contradictory results for the angular distribution of the inelastically scattered at lowest-lying levels in ^{28}Si neutrons. This may clearly results from experimental difficulties not included in the errors given by the authors arising from problems of peak identification and separation.

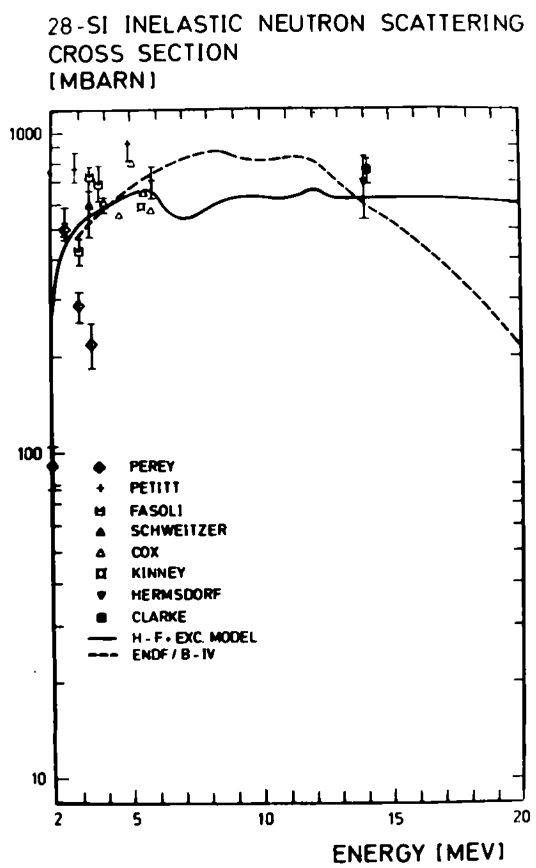

Fig. 6

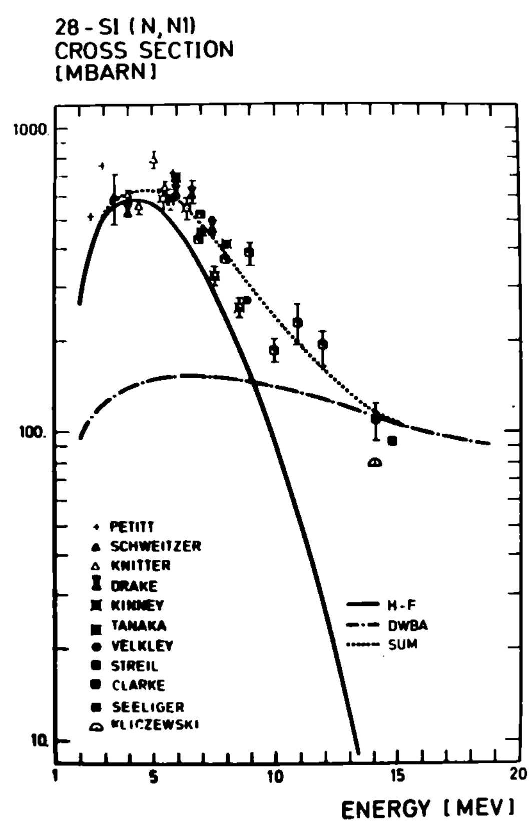

Fig. 7

2.2. Theoretical interpretation of inelastic neutron scattering

2.2.1. Statistical model calculations

Commonly neutron inelastic scattering exciting the lowest-lying levels can be understood well from threshold up to about 5 MeV in terms of the Hauser-Feshbach-formalism uncluding width-fluctuation correction. To obtain reliable results, as much as possible reaction channels energetically possible for the de-excitation of the compound nucleus should be taken into account. Because of the highly resolved level scheme of nuclei in this mass range roughly 60 discrete particle transitions has to be incorporated in a Hauser-Feshbach calculation (see tables 2 and 3).

The code ELIESE-III /33/ is limited to 30 discrete levels only but a nuclear level density can be introduced for that residual nucleus giving the most important contribution to the Hauser-Feshbach denominator (normalization factor). This limitation can be eluded using the code STAPRE /38/ suffering the loss of angular distribution informations.

Combining the results obtained using both codes, the excitation functions and angular distributions of 17 lowest-lying levels of ^{28}Si have been evaluated.

Above 5 MeV deviations appear indicating contributions from reaction modes other than statistical ones (see for example fig. 6). Usually collective reactions are held to be responsible for this.

2.2.2. Direct reactions calculations

Pronounced deviations from statistical model predictions can be seen in experiments as well as in shape of angular distributions and excitation functions at higher energies. Streil /17/ has found a contribution of direct inelastic neutron scattering of 40 % for $^{28}Si(n,n_1)$ at 7 MeV (see fig. 7).

This author has investigated in detail direct reaction excitation of low-lying levels in ^{28}Si. Basing on collective models and further refinements by taking into account channel coupling, absolute differential cross sections have been calculated using a slightly changed optical potential (table 1) and coupling strenghts for quadrupole and hexadecapole deformations β_2 and β_4 respectively /17/. The calculations were carried out by the CCBA code CHUCK /39/. All results have been adopted from ref. /17/.

The understanding of the angular distributions of inelastically scattered neutrons is excellent using an incoherent superposition of statistical and direct reaction contributions. For example see fig. 8.

Fig. 8

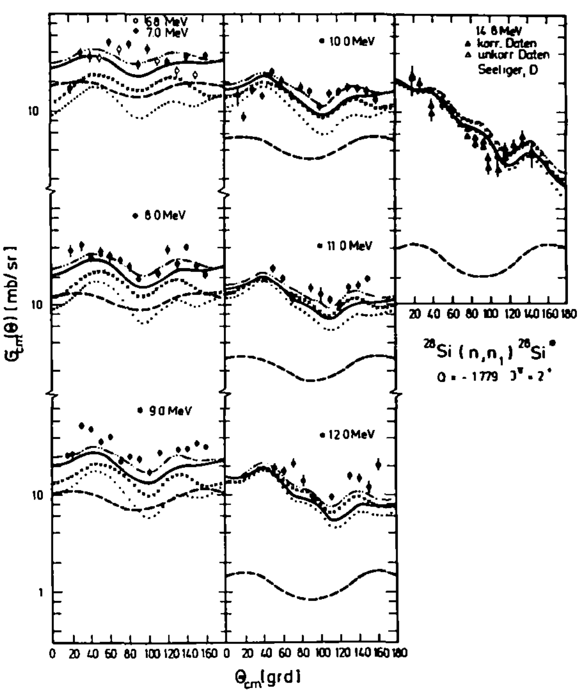

Neutron inelastic scattering exciting low-lying levels in ^{29}Si is of minor interest. Nevertheless, excitation functions for the first few levels have been compiled. By the absence of any experiment they are basing on statistical model calculations only. Therefore, all angular distributions are symmetric around 90 degrees. Calculations done by ELIESE agree very well with that evaluated in MAT 1194 of ENDF/B-IV, which has been adopted without change for the present evaluation.

2.2.3. Calculation of inelastic scattering to highly excited states in Si (level continuum)

Excitation functions of highly excited states or inelastic scattering to the level continuum can be reasonable described by the statistical model because of negligible contributions from collective reactions.

On the other hand, pre-equilibrium reactions enhance the emission of high energetic neutrons observed really in experiments /40/. So, the spectrum of neutrons emitted following inelastic scattering may be composed of contributions from compound and pre-equilibrium reactions.

Using the code STAPRE /38/ neutron evaporation and neutron pre-equilibrium emission can be calculated. The calculations basing on the Exciton model using $|M|^2 = 95\ E^{-1}\ A^{-3}$ as optimum value for the matrix element.

By this way, the spectra of primary emitted neutrons including also contributions from $(n,n'p)$ and $(n,n'\alpha)$ reactions have been estimated. In fig. 9 an example will be given.

Commonly, angular distributions of neutrons inelastically scattered at highly excited levels should be assumed to be isotropic following statistical nuclear reaction mechanism conceptions. The essential component of pre-equilibrium processes in inelastic neutron scattering can be seen in the total neutron inelastic scattering cross section shown in fig.6.

Fig. 9

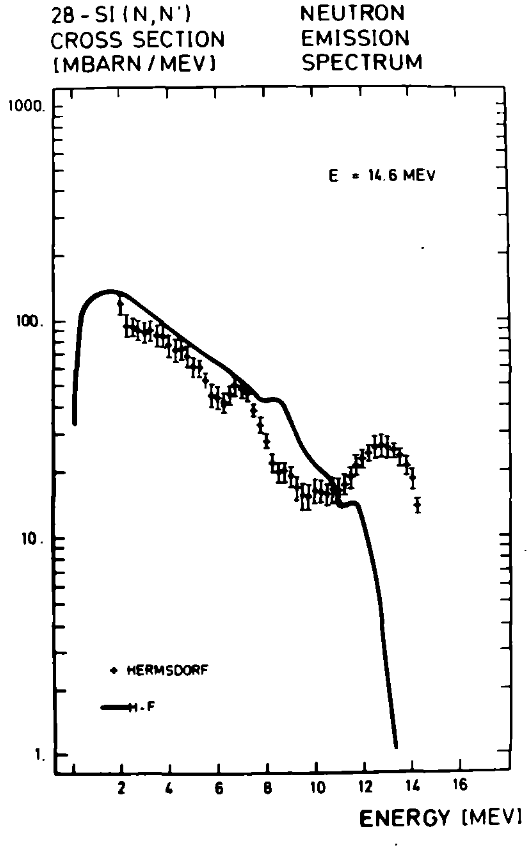

Such calculations can be carried out correctly only taking into account all competing channels besides neutron emission, i.e. charged-particle and γ-ray emission and multi-step-reactions also. Therefore, all spectroscopic informations of tables 2 and 3 supplemented by level-density parameters compiled in table 4 are necessary to complete input data for statistical model calculations. These parameters have been adjusted by an empirical method proceeding from back-shifted-Fermigas-model parameters published by Beckerman /41/ and Dilg /42/.

3. Secondary neutron production cross sections

3.1. Si(n,2n) cross sections

3.1.1. Review of experimental data

Si (n,2n) cross sections may be determined to come from ^{29}Si below 18 MeV neutron incident energies because of very different Q-values of ^{28}Si ($Q_{n,2n}$= -17.2 MeV) and ^{29}Si ($Q_{n,2n}$=-8.5 MeV). As well as concerning $^{29}Si(n,2n)$ and $^{28}Si(n,2n)$ only very scarce experimental data are available. These results /43/ were used to adjust the predicted by STAPRE values of (n,2n) reaction cross sections.

3.1.2. Theoretical calculations of Si(n,2n)

Calculations were carried out using the code STAPRE. The excitation function of Si(n,2n) has been superimposed from weighted (according to the isotropic composition) cross sections of $^{29}Si(n,2n)$ and $^{28}Si(n,2n)$.

Spectra of secondary neutron emission will arise only above 20 MeV taking into account transitions to isolated low-lying levels in the residual nuclei ^{28}Si and ^{27}Si. Therefore they are absent in the evaluated nuclear data file discussed here.

3.2. Si(n,pn) and Si(n,αn) cross sections

Secondary neutron spectra arising from multi-particle-emission reactions (n,pn) and (n,αn) may also be predicted by statistical model calculations using the code STAPRE.

Because of the absence of any experimentally determined value as well as in excitation function and particle spectrum, all calculations may be regarded as speculative within the validity of the model applied.

For completeness they have been included in the present evaluation.

4. Miscellaneous quantities of neutron scattering cross sections

Further quantities related to neutron scattering have not been included in the present evaluation. Especially, if there arise requests concerning averaged properties of elastic neutron scattering we refer to common relations to have to apply to get

i) the average cosine of the scattering angle for elastic scattering (in the lab-system)

$$\bar{\mu}_{Lab} = f_1^{Lab}(E)$$
$$= \sum_{m=0}^{NM} f_m^{CM}(E)\, U_{1,m}$$

using the transformation matrix elements $U_{1,m}$ and Legendre-polynomial-expension coefficients f_m (in the CM-system) compiled in file 4.

ii) the average logarithmic energy decrement for elastic scattering

$$\xi = \xi_o - 3\,\bar{\mu}_{CM}\left[\frac{1}{1-a} - \frac{3}{2} + \xi_o\right]$$

with $\xi_o = 1 + \dfrac{a}{(1-a)^2}\ \ln a$ and $a = \left(\dfrac{A-1}{A+1}\right)^2$

iii) the average of the square of the logarithmic energy decrement for elastic scattering, divided by twice the average logarithmic energy decrement

$$\gamma = \overline{\xi^2}/2\xi$$

All data necessary for calculations can be obtained from MF=4 MT=2.

5. References

/1/ G.V. Lovchikova et al., EXFOR acc. no. 80056

/2/ W.E. Kinney et al., report ORNL-4517, 1970

/3/ R.O. Lane et al., Ann. Phys. 12 (1961) 135

/4/ S.A. Cox et al., EXFOR acc. no. 11519

/5/ I.O. Korzh, EXFOR acc. no. 80197

/6/ T. Schweitzer, S. Unholzer, Thesis, TU Dresden, 1978

/7/ G.A. Petitt et al., Nucl. Phys. 79 (1960) 231

/8/ V. Fasoli et al., report EANDC (E) 66, 1966

/9/ V.I. Popov et al., EXFOR acc. no. 80327

/10/ H.H. Knitter et al., Z. Phys. 207 (1967) 56

/11/ K. Tsukada et al., EXFOR acc. no. 20341

/12/ W.E. Kinney et al., EXFOR acc. no. 10107

/13/ W.M. Currie et al., report AERE-PR/NP-9, 1966

/14/ D.M. Drake et al., EXFOR acc. no. 51828

/15/ S. Tanaka et al., EXFOR acc. no. 20343

/16/ S. Grimes et al., EXFOR acc. no. 10012

/17/ Th. Streil, Thesis, TU Dresden, 1981
D. Schmidt, D. Seeliger, Th. Streil, ZfK-459, 1981, p. 164, INDC(GDR)-19/G, 1982

/18/ D. Brandenberger et al., Nucl. Phys. A196 (1972) 65

/19/ Mittler et al., EXFOR acc. no. 50301

/20/ D.E. Velkley et al., Phys. Rev. C9 (1974) 2181

/21/ A.W. Obst, J.L. Weil, Phys. Rev. C7 (1973) 1076

/22/ J. Rapaport et al., Nucl. Phys. A286 (1977) 232

/23/ M. Joppich, Thesis, Univ. Erlangen, 1974

/24/ J. Höhn et al,, Nucl. Phys. A134 (1969) 289

/25/ S. Kliczewski, J. Lewandowski, Nucl. Phys. A304 (1978) 269

/26/ J. Roturier et al., EXFOR acc. no. 60162

/27/ P.H. Stelson et al., Nucl. Phys. 68 (1965) 97

/28/ R.L. Clarke et al., Nucl. Phys. 53 (1964) 177

/29/ I. Schouky, report KfK-2503, 1977

/30/ D.J. Bredin et al., Phys. Rev. B135 (1964) 412

/31/ M.R. Bhat et al., report BNL-50379, 1973

/32/ B. Holmqvist, T. Wiedling, J. Nucl. Energy 27 (1973) 543

/33/ S. Igarasi, report JAERI-1224, 1972

/34/ F.G. Perey et al., EXFOR acc. no. 52216

/35/ D. Sullivan et al., Nucl. Sci. Eng. 70 (1979) 294

/36/ D. Hermsdorf et al., Kernenergie 18 (1975) 83

/37/ P.M. Endt, C. van der Leun, Nucl. Phys. A310 (1978) 1

/38/ M. Uhl, B. Strohmaier, report IRK-76/1, 1976

/39/ P.D. Kunz, private communication

/40/ K. Seidel, D. Seeliger, R. Reif, V.D. Toneev, ECHAYA 7 (1976) 13

/41/ M. Beckerman, Nucl. Phys. A278 (1977) 333

/42/ W. Dilg, W. Schantl, H. Vonach, Nucl. Phys. A217 (1973) 269

/43/ Arnold et al., EXFOR acc. no. 11520

6. Tables

Table 1: Optical potential well parameters for $^{28}Si+n$. Energies are in MeV, radii and diffusenesses in fm. The form factors are of Woods-Saxon and derivative Woods-Saxon type for the real and imaginary well respectively.

Parameter	Bhat /31/	Holmqvist /32/ *	Kliczewski /25/**	Obst /21/***	present work H-F	present work CCBA/17/
V_R	56.3-0.32E	48.5	43.13	52.0	52.0	52.0
r_R	1.17	1.191	1.27	1.15	1.15	1.15
a_R	0.75	0.66	0.68	0.78	0.78	0.78
W_I	13.0-0.25E	7.89	9.63	12.1	12.1	0.57E+0.26
r_I	1.26	1.201	1.23	1.25	1.25	1.25
b	0.58	0.48	0.45	0.47	0.47	0.47
V_{so}	6.2	8.0	8.91	4.9	9.0	4.9

* valid at 8 MeV
** valid at 14 MeV
*** valid at 10 MeV

Table 2: Spectroscopic data of the discrete levels in Silicon isotopes used for theoretical interpretation /37/

Level no.	^{28}Si Excitation energy/MeV	I^{π}	^{29}Si Excitation energy/MeV	I^{π}	^{30}Si Excitation energy/MeV	I^{π}
1	0.0	0^+	0.0	$1/2^+$	0.0	0^+
2	1.78	2^+	0.75	$1/2^+$	2.23	2^+
3	4.62	4^+	1.69	$5/2^+$	3.51	2^+
4	4.98	0^+	2.32	$3/2^+$	3.77	1^+
5	6.28	3^+	2.79	$5/2^+$	3.79	0^+
6	6.69	0^+	3.14	$7/2^-$	4.81	2^+
7	6.88	3^-	3.53	$3/2^-$	4.83	3^+
8	6.89	4^+	3.88	$7/2^+$	5.23	3^+
9	7.38	2^+	4.26	$3/2^+$	5.27	4^+
10	7.42	2^+	4.38	$3/2^-$	5.37	0^+
11	7.80	3^+			5.49	3^-
12	7.93	2^+			5.61	2^+
13	8.26	2^+			5.95	4^+
14	8.33	2^+			6.50	4^-
15	8.41	4^+			6.54	2^+
16	8.54	6^+			6.63	0^+
17	8.59	3^+			6.74	1^-
18	8.90	1^-			6.86	3^+
19					6.91	2^+
20					7.00	3^+

Table 3: Spectroscopic data of discrete levels in residual nuclei formed by neutron-induced reactions on Silicon /37/

	^{28}Al		^{25}Mg		^{27}Al	
Level no.	Excitation energy/MeV	I^{π}	Excitation energy/MeV	I^{π}	Excitation energy/MeV	I^{π}
1	0.0	3^+	0.0	$5/2^+$	0.0	$5/2^+$
2	0.03	2^+	0.59	$1/2^+$	0.84376	$1/2^+$
3	0.97	0^+	0.97	$3/2^+$	1.0145	$3/2^+$
4	1.01	3^+	1.61	$7/2^+$	2.2105	$7/2^+$
5	1.37	1^+	1.96	$5/2^+$	2.7344	$5/2^+$
6	1.62	1^+	2.56	$1/2^+$	2.9811	$3/2^+$
7	1.63	2^+	2.74	$7/2^+$	3.0042	$9/2^+$
8	2.14	2^+	2.80	$3/2^+$		
9	2.20	1^+	3.40	$9/2^+$		
10	2.27	4^+	3.41	$3/2^-$		
11	2.49	2^+	3.91	$5/2^+$		
12	2.58	5^+	3.97	$7/2^-$		
13	2.66	4^+	4.06	$9/2^+$		
14			4.28	$1/2^-$		
15			4.36	$3/2$		
16			4.71	$9/2^+$		
17			4.72	$1/2^-$		
18			5.01	$7/2^-$		

Table 4: Level-density parameters of back-shifted-Fermi-gas-model used in STAPRE calculations (the moment of inertia has been assumed to be that of the rigid body)

Nucleus / Quantity	^{29}Si	^{28}Si	^{27}Si	^{28}Al	^{27}Al	^{26}Al	^{25}Mg	^{24}Mg
a/MeV^{-1}	3.5	4.0	4.5	4.0	3.0	3.0	4.5	3.0
Δ/MeV	0.5	1.0	-2.5	-4.0	-2.0	-3.5	-2.5	2.0

7. Figure captions

Fig. 1 Silicon neutron elastic scattering and inelastic scattering to the first excited level.
Experimental data obtained by Schouky /29/ for (n,n) and Sullivan /35/ for (n,n_1) are compared to predictions of the optical model for (n,n) and the statistical model for (n,n_1). For further explanation see also fig. 12 of part B.

Fig. 2 Silicon neutron elastic scattering.
In the energy range from 1 to 20 MeV the experimental data scatter considerably. The optical model prediction (solid line) passes through the data points. Contributions from compound elastic scattering decrease with increasing energy (dashed line).

Fig. 3 Silicon neutron elastic scattering.
The angular distribution of elastically scattered neutrons of 5 MeV can be reasonable interpreted by the optical model calculation (solid line).

Fig. 4 Same as in fig. 3 for 20 MeV neutrons.

Fig. 5 Same as in fig. 3 for 26 MeV neutrons.

Fig. 6 Silicon neutron inelastic scattering.
Scarce and contradictory experimental data for total inelastic scattering cross sections can be interpreted by the statistical model including (solid line) and without preequilibrium emission (dashed line).

Fig. 7 Silicon neutron inelastic scattering.
The excitation function for the first level in ^{28}Si by neutrons can be understood in terms of a superposition of statistical model (solid line) and direct reaction (dashed-dotted line) contributions.

Fig. 8 Silicon neutron inelastic scattering.
The angular distributions of neutrons exciting the first level in ^{28}Si at different neutron incident energies are always consistently interpreted by a sum of statistical (dashed lines) and direct reaction (dotted lines and crosses) contributions. Experimental as well as theoretical data are taken from Streil /17/.

Fig. 9 Silicon neutron emission spectrum.
The neutron emission spectrum induced by 14-MeV incident neutrons exhibits deviations from compound nucleus reaction model calculations (solid line) caused by pre-equilibrium processes.

Part D:

Neutron-induced charged-particle production cross sections

D. Hermsdorf

This part has been published separately as report INDC(GDR)-22.

Part E:

γ-ray production cross sections

D. Hermsdorf, E. Paffrath

1. Neutron capture

1.1. Review of experimental data

Only very few informations can be obtained from compilations of experimental data for neutron capture. At about $2 \cdot 10^{-2}$ eV two measurements have been carried out /1, 2/ useful for the adjustment of the 1/v-law describing the thermal energy range.

At higher energies very discrepant data have been published /3, 4, 5/ in the keV range. Further only at 14 MeV measurements have been reported /6 to 11/ inclusive the capture γ-ray spectrum /7/.

From this insufficient knowledge any evaluation must rely upon more or less substantiated calculations resulting in very different recommended data sets seen in fig. 1

Fig. 1

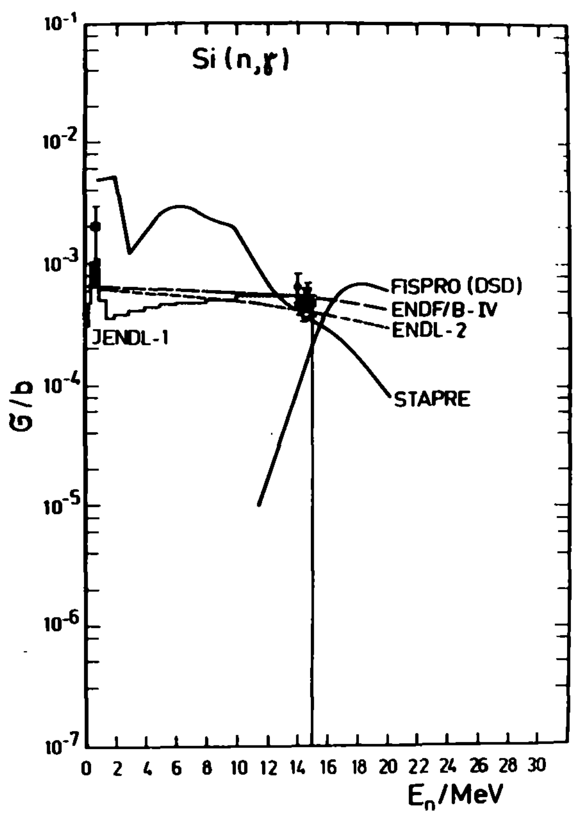

1.2. Theoretical description of neutron capture

1.2.1. Thermal neutron capture

In the absence of bound levels or/and capture resonances at thermal energies the simple 1/v-law should be fulfilled. Assuming this the capture cross section for Si has been determined to be

$$\sigma_{n,\gamma}^{thermal} = 0.023506/\sqrt{E/eV} ,$$

which should be valid up to about 10 keV.

1.2.2. Resonance capture

In the energy range 100 keV to 1.56 MeV neutron capture cross sections were calculated taking the resonance parameters compiled in table 2 of Part B and the Single-Level-Breit-Wigner-formalism. The results obtained were matched to the 1/v-law at about 10 keV and calculations carried out using statistical models above 1 MeV.

1.2.3. Fast neutron capture

It is a well-established fact that the de-excitation of a highly exited nucleus by γ-rays can be understood in terms of the statistical model also taking into account competing other reaction channels (neutron emission channels mainly). Generally, a very reasonable description can be achieved by taking the strongest multipole order of electromagnetic radiation E1 only.

Some practicable computer codes basing on this formalism exist at present. In this work the codes FISPRO /12/ and STAPRE /13/ have been applied. Starting from well approved parameters fitting particle channels simultaneously, radiation widths and E1-strength functions a reasonable interpretation of the scarce experimental data base is possible from the keV-range up to about 10 MeV. Difficulties arise above 10 MeV coming from the fact that neutron capture may proceed via more direct processes.

Direct capture modes have been estimated using the code FISPRO which incorporates the Direct-Semidirect model. In the frame of this model the "collapse" of capture cross section above 10 MeV may be stopped really but the spectrum of γ-rays emitted will not described correctly.

Therefore, attempts have been undertaken to calculate γ-ray spectra using a pre-equilibrium model for γ-ray emission elaborated by Bĕták /14/.

Fig. 2

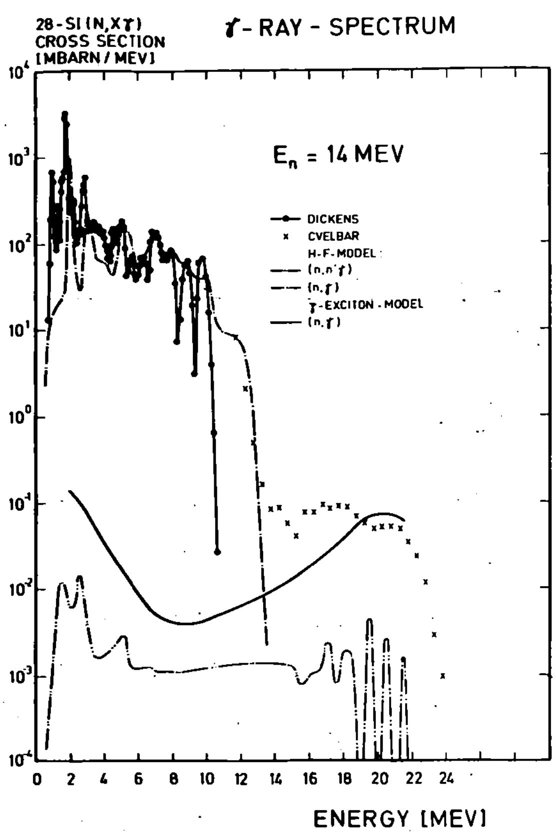

Details of the model and encouraging results obtained by the relevant code PQGM /15/ have been published recently by the authors /16/. Fig. 2 shows the results at 14 MeV.

1.3. Conclusions and recommendations

Combining theoretical calculations predicted by quite different capture reaction mechanism models the reliability of recommended cross sections as well as γ -ray spectra and integral ones should be improved.

The representation of integral capture cross sections is divided into three energy ranges mentioned above already: the thermal region, the resonance region and the fast neutron region up to 20 MeV.

γ-ray spectra calculated by PQGM or STAPRE have been included.

Following the suppositions of the models applied only isotropic angular distributions for emitted γ-rays can be expected.

2. γ-ray emission from neutron inelastic scattering

2.1. Emission of discrete γ-lines

2.1.1. Review of experimental data

γ -ray transitions between low-lying levels in ^{28}Si excited by neutron inelastic scattering is studied reasonable well.

Excitation functions for several discrete γ-lines were measured by numerous authors /17 to 27/. An example is given in Fig. 3 showing the most dominant line with E_{γ} = 1.78 MeV arising from the de-excitation of the 2_1^+ state in ^{28}Si.

Also a few experiments have been reported on discrete γ-lines arising from transitions between excited states in ^{29}Si and ^{30}Si /26, 28/.

Fig. 3

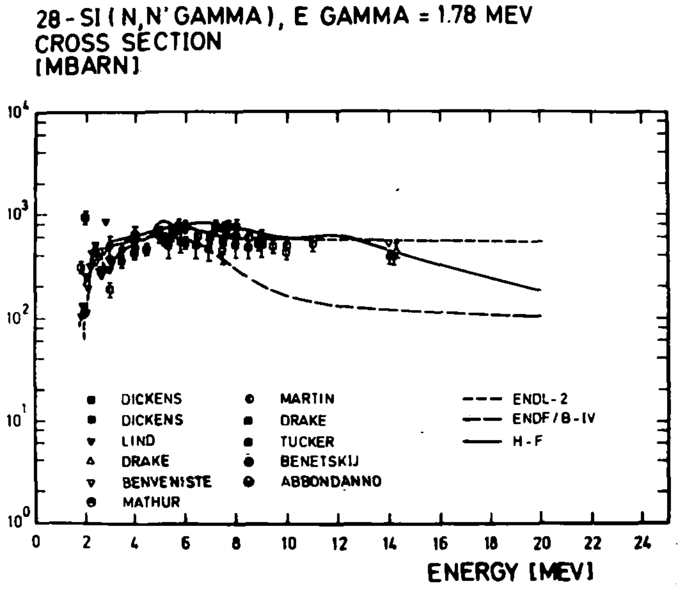

2.1.2. Theoretical interpretation

A surprisingly good description of excitation functions for γ-transitions between discrete levels in the nucleus excited by neutron inelastic scattering can be obtained from STAPRE code. In this way basing on adjusted parameters and branching ratios taken from Endt and von der Leun /29/. Demonstrating the reliability of choosen parameters fig. 3 shows experimental as well as theoretical results.

By this method excitation functions for 19 discrete γ-lines emitted from ^{28}Si and ^{29}Si have been recommended in this work. Only slight adjustments were necessary to improve the agreement of experimental data for transitions between higher-excited levels.

2.2. Continuous γ-ray spectra

2.2.1. Review of experimental data

Up to an incident neutron energy of about 10 MeV the continuously distributed γ-ray emission will arise from neutron inelastic scattering to the level continuum in target nucleus.

In the energy range from 1.25 MeV to 20 MeV Dickens et al. /19/ have measured γ-ray spectra at different angles of γ-ray emission. The spectra clearly show the typical superposition of discrete lines and continuous γ-ray-"background". The accuracy of such measurements are limited principally by spectra unfolding methods to have to applied and decreasing detection efficiencies with increasing γ-ray energies.

Therefore, the structure seen in experimental spectra (figs. 2 and 4) may not be realistically at all.

Fig. 4

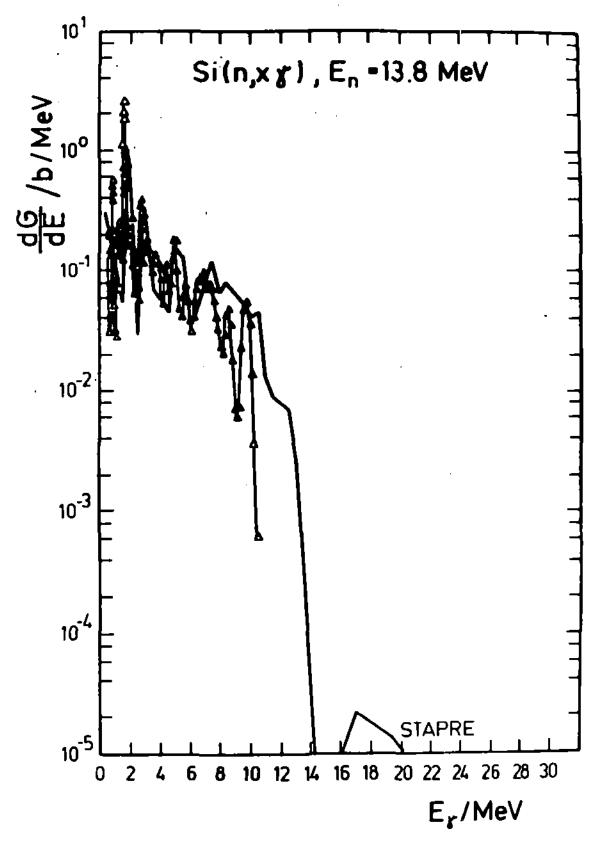

2.2.2. Theoretical interpretation

The emission of a continuously distributed in energy γ-rays can be described by the γ-ray-cascade-model also included in STAPRE. Parameters inherent to this model the γ-ray transmission coefficients appear approximated by the Brink-Axel approach for E1 /30/ and simple Weisskopf estimates for all higher order multipoles.

Generally, this model yields surprisingly good results shown for example in figs. 2 and 4.

2.3. Conclusions and recommendations

The success of the model used in STAPRE allows to calculate all spectra compiled in the recommended data file for Silicon under discussion here.

3. γ -ray production cross sections

3.1. Review of experimental data

In the fast neutron energy range the neutron-induced γ-ray emission is mainly due to neutron inelastic scattering. Contributions from reactions (n,γ), $(n,p\gamma)$, $(n,\alpha\gamma)$, $(n,2n\gamma)$ and other ones are present above 10 MeV practically but they are smaller than $(n,n'\gamma)$ at least by one order of magnitude or more /16, 31/.

From experimental point of view, γ-quanta emitted cannot be distinguished with the exception only they can be identified to come from transitions between strongly excited discrete levels in a residual nucleus. Therefore, γ-ray spectra measured at neutron energies above 10 MeV /19/ are γ -ray production spectra (for example see fig. 2).

Integrating these spectra γ-ray production cross sections can be determined with a rather limited accuracy only.

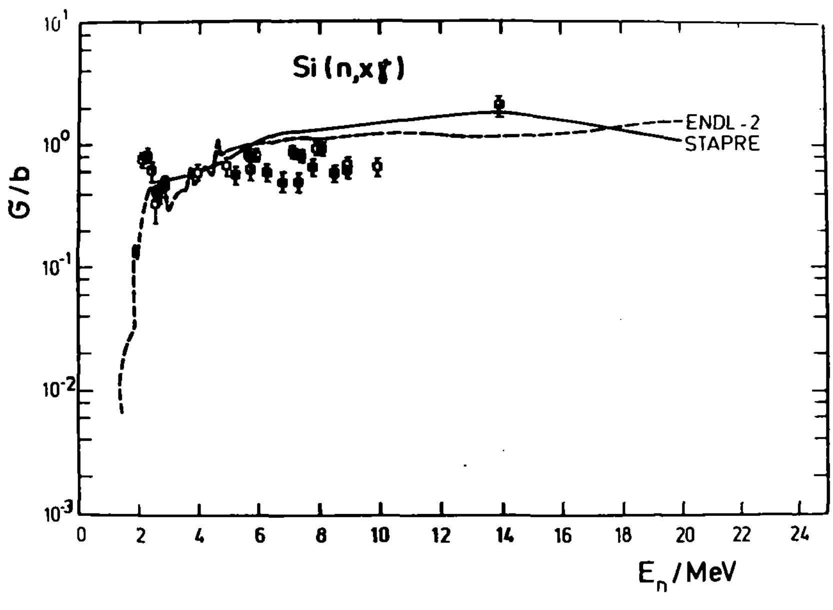

Fig. 5

At lower neutron energies the production cross section may be composed of the individual excitation functions for the emission of discrete γ-lines. Fig. 5 shows compiled experimental data as well as theoretical ones.

3.2. Theoretical interpretation

In the same manner the (n,n'γ) cross sections have been determined the other reactions of interest can also calculated. Doing this using code STAPRE we start from well-established parameters resulting from the adjustment of particle emission reaction channels simultaneously. The results obtained are included in figs. 2, 4 and 5.

A satisfactory agreement should be noted for all quantities comparable to experimental data. So, a large amount of unmeasured data have been predicted theoretically to be incorporated in the present evaluation.

4. Conclusions and recommendations

The evaluated data file discussed here contains an extended data set for γ-ray cross sections produced by incident neutrons. As well as integrated cross sections (excitation functions for 19 discrete γ-rays from ^{28}Si and ^{29}Si) and γ-ray spectra are included.

Because all theoretical models applied to estimate cross sections cannot calculate angular distributions of γ-ray emission these have assumed to be isotropic in acceptable agreement with scarce experimental informations.

5. References

/1/ A.M.J. Spits et al., Nucl. Phys. A224 (1974) 517

/2/ A.M.J. Spits et al., Nucl. Phys. A145 (1970) 449

/3/ anonym, EXFOR acc. no. 80320.003

/4/ R.L. Macklin et al., Phys. Rev. 129 (1963) 2695

/5/ J.H. Gibbons et al., Phys. Rev. 122 (1961) 182

/6/ F. Rigaud et al., Nucl. Phys. A154 (1970) 243

/7/ F. Cvelbar et al., Nucl. Phys. A138 (1969) 412

/8/ A. Hudoklin-Bozic et al., report NIJS-P-213, 1968

/9/ F. Budnar et al., report INDC (YUG)-6/L, 1979

/10/ F. Csikai et al., Nucl. Phys. A95 (1967) 229

/11/ J.L. Perkin, Proc. Phys. Soc. 72 (1958) 505

/12/ V. Benzi et al., report RT/FI (69) 44, 1969

/13/ M. Uhl, B. Strohmaier, report IRK-76/01, 1976

/14/ E. Běták, J. Dobeš, Phys. Lett. 84 B (1979) 368

/15/ E. Běták, private communication, 1981

/16/ B. Basarragtscha, D. Hermsdorf, E. Paffrath, J. Physics G: Nucl. Phys. 8 (1982) 275

/17/ W.E. Tucker et al., report DASA-2333, 1969

/18/ J.K. Dickens et al., Phys. Rev. C2 (1970) 990

/19/ J.K. Dickens, T.A. Love, G.L. Morgan, Phys. Rev. C 10 (1974) 958

/20/ D.M. Drake et al., Nucl.Science Eng. 40 (1970)

/21/ P.T. Martin et al., J. Nucl. Energy 19 (1965) 447

/22/ S.C. Mathur et al., Nucl. Phys. 73 (1969) 561

/23/ U. Abbondanno et al., J. Nucl. Energy 27 (1973) 227

/24/ B.A. Benetskii et al., EXFOR acc. no. 80256.003

/25/ J. Benveniste et al., report UCID-4619, 1963

/26/ D.A. Lind, R.B. Day, Ann. Physics 12 (1961) 485

/27/ T. Roturier, EXFOR acc. no. 20599.014

/28/ D.M. Drake et al., Nucl. Phys. A128 (1969)

/29/ P.M. Endt, C. van der Leun et al., Nucl. Phys. A 310 (1978)1

/30/ P. Axel, Phys. Rev. 126 (1962) 671

/31/ B. Basarragtscha, D. Hermsdorf, D. Seeliger, Proc. 2nd Int. Symp. on Neutron-Induced Nuclear Reactions, Smolenice, 1979, in Physics and Applications, Vol. 6, p. 381, Bratislava, 1980

6. Figure captions

Fig. 1 Silicon neutron capture cross sections.
Calculations by STAPRE and FISPRO of the present work are compared with evaluations from ENDL and ENDF/B-libraries.

Fig. 2 Silicon neutron-induced γ-ray spectrum.
The γ-ray spectrum produced by 14-MeV neutrons impinging on Si is composed of components coming from neutron capture (n,γ), inelastic neutron scattering $(n,n'\gamma)$ and other nonelastic processes like $(n,\alpha\gamma)$ and $(n,p\gamma)$.

Fig. 3 Excitation function of the 1.78 MeV γ-line from Silicon.
Experimental results can be described in terms of statistical models for neutron and γ-ray emission.

Fig. 4 γ-ray spectrum induced by neutron nonelastic processes at 13.8 MeV incident energy.
Experimental data are described by statistical models.

Fig. 5 Silicon γ-ray production cross sections.
Calculations by STAPRE done in the present work are compared with experimental data and the evaluation ENDL-2.